Transition from clustered state to spatiotemporal chaos in a small-world networks

Ashwini V. Mahajan[1] and Prashant M. Gade[2]

[1]*Centre for Modeling and Simulation, University of Pune, Pune 411007, India*
[2]*PG Department of Physics, Rashtrasant Tukdoji Maharaj Nagpur University, Nagpur 440033, India*

We study the spatiotemporal patterns in coupled circle maps on a small-world network. This system shows a rich phase diagram with several interesting phases. In particular, we make a detailed study of transition from clustered phase to spatiotemporal chaos. In the clustered state, observed at smaller coupling values, some sites stay close to the fixed point forever while others explore a larger part of the phase space. For stronger coupling, there is a transition to spatiotemporal chaos where no site stays close to fixed point forever. We study this transition as a dynamic phase transition. Persistence acts as a good order parameter for this transition. We find that this transition is continuous. We also briefly discuss other phases observed in this system.

I. INTRODUCTION

Of late, spatially extended dynamical systems have been a subject of intensive research. Partial differential equations [1], oscillator arrays [2], coupled map lattices [3], and cellular automata [4] are the main paradigms in these studies and all these approaches have given some useful information in understanding these systems. After low dimensional chaotic systems were reasonably well understood, there has been an extensive work attempting to understand spatially extended nonlinear systems. One of the simplest and popular attempt to build spatially extended systems using low dimensional systems as building blocks has been coupled map lattice (CML) [5]. While we observe several different dynamic phases ranging from stripes to spirals in real systems, the most commonly explored theme in recent literature studying oscillator arrays and coupled map lattices has been that of synchronization [6]. Though it is an important feature, synchronized state is a minuscule part of the phase space of these systems. Other dynamic phases have been studied much less and deserve further attention.

In general, these systems are studied on *d*-dimensional regular Cartesian lattice with diffusive or nonlinear coupling. Most studies are about logistic maps, but there have been studies on other maps such as coupled circle maps. In coupled circle maps, a remarkable variety of behaviors is observed ranging from synchronization, spatiotemporal intermittency, spatial intermittency, traveling waves, etc. They also found an evidence of directed percolation (DP) universality class in transition from laminar state to spatiotemporal intermittency [7–11]. In coupled maps apart from *d*-dimensional lattices, fully global coupling is also investigated in few cases [12]. However, several other topologies are relevant in different contexts and have not been given due attention. Apart from theoretical interests, these topologies are inspired by real life situations such as biological systems. Biological systems such as neuronal networks or food webs do not sit on a *d*-dimensional regular lattice since these systems have a complex architecture which is not yet clearly understood. Only recently, we have an extensive data in this regard and various computational models have been proposed to explain the structure of such networks.

Two of the most extensively studied models have been the small-world networks [13] and the scale-free networks [14]. The geometrical properties of these networks and their robustness with respect to perturbations have also been studied extensively [15]. Most prominent difference in these two models is about their degree distribution. As the name implies, scale-free networks display a power-law degree distribution while small-world models show an exponential decay for larger degrees. Barabási-Albert (BA) model has been most popular algorithm for generating scale-free models. In this model, average path length grows logarithmically with number of sites (with a double logarithmic correction) and is systematically shorter than random graph. Small-world networks approach random graph in the limit $p \rightarrow 1$. However, average path length for small-world network approaches that of random graph for very small values of rewiring probability p. Thus, due to nonlocal connectivities, the average path length of scale-free or small-world networks (even for small values of p) is much smaller than a *d*-dimensional lattice. The clustering coefficient for small-world networks remains very high for small values of p and decays to the value in random networks for large values of p. It is independent of number of sites. On the other hand, the clustering coefficient in BA model scales with network size and is higher than random networks. Several variants of these models have been proposed and studied. These are highly nonlocal models. In statistical physics, it is well known that networks with highly nonlocal connections such random nonlocal coupling or Cayley-tree-like coupling or coupling which decays very slowly, exhibits mean-field-like properties [16]. One would expect a similar behavior in small-world or scale-free systems. However, the behavior could be markedly different since dynamical time scales play as important a role as topology in these systems [17]. Nevertheless, it could be said that dynamics on such systems (apart from the stability of a synchronized state) is much less studied. In the initial studies, it was thought that some very interesting properties will emerge in small-world networks even in the limit $p \rightarrow 0$. It was found to be true in models in equilibrium statistical physics such as Ising model, *XY* model, or a percolation problem (see, e.g., [18–22]). These are not dynamical systems in the strict sense of the word. However, in dynamical systems, the changes are more gradual and it has been shown

that topology alone does not decide the nature of asymptotic phase in these systems. (see, for example, [17,23,24]) Changes are gradual and no surprising changes occur for $p \rightarrow 0$ [25].

Here, we study phase diagram of coupled circle maps on a small-world network. Circle map is a mathematical model that exhibits the phenomenon of frequency-locking. In fact, it is a standard model displaying the characteristic features of quasiperiodic route to chaos. It is an iterated map and the iterated variable is interpreted as the measure of angle that specifies where the trajectory is on a circle [26,27]. We observe spatiotemporal behavior in coupled circle maps and report several interesting phases. In particular, we follow Watts-Strogatz construction of small-world network in which L sites on a circle are placed and connected with m neighbors on either side. Later, the connections are disconnected from a given site i with probability p and replaced with nonlocal connections. In a variant of this model by Newman and Watts, instead of rewiring links between sites chosen at random, extra links are added between pairs of sites chosen at random without removing links from underlying lattice [28]. Recently, Kleinberg studied a model in which the nonlocal connections are chosen with a distance-dependent probability [29]. We restrict our studies to original model by Watts and Strogatz. In particular, we make a detailed study the transition from clustered state to spatiotemporal chaos as a dynamic phase transition. This is a transition from localized to spatiotemporally chaotic state. We analyze this transition as a nonequilibrium phase transition and propose persistence as an order parameter to quantify the transition.

II. MODEL

Let $i=1,2,\ldots,L$ be L sites on a circle. Let $x_i(t)$ be a continuous variable associated with site i at time t. We construct a Watts-Strogatz small-world network on these sites. Each site has two nearest neighbors on either side, i.e., $m =2$. This gives us $2m$ connections. We disconnect the connection from any site to its nearest neighbors with probability p and rewire it by connecting it to a randomly chosen site. Boundary conditions are periodic. The evolution of $x_i(t)$ is defined as

$$x_{i,t+1} = (1 - \epsilon)f(x_{i,t}) + \frac{\epsilon}{4}\{f(x_{\xi_1(i),t}) + f(x_{\xi_2(i),t}) + f(x_{\xi_3(i),t})$$

$$+ f(x_{\xi_4(i),t})\}, \qquad (1)$$

where t is discrete time index and ϵ is the coupling strength among the lattice sites in the interval $[0,1]$. We define, $\xi_1(i)=i+1$, $\xi_2(i)=i+2$, $\xi_3(i)=i-1$, $\xi_4(i)=i-2$ with probability $1-p$. Otherwise, they can take a uniformly distributed random integer value in the interval 1 and L with probability p. The connections are quenched, i.e., they are made in the beginning of a simulation and retained throughout. However, for each configurations, we change connections as well as initial conditions. Thus, we have done averaging over initial conditions as well as the connectivities in the results given below. We have also carried out averaging over initial conditions alone and as expected results do not change for large

enough lattice. Four neighbors are used in order to avoid a possible formation of isolated cluster due to nonlocal connections. The $p=0$ case corresponds to nearest and next-nearest couplings for each site on a circle.

The local on-site map $f(x)$ is the sine circle map defined as

$$f(x) = x + \omega - \frac{k}{2\pi}[\sin(2\pi x)], \qquad (2)$$

where ω is the winding number and parameter k denotes the nonlinearity. This map shows a very interesting and unexpected behavior. For $k=0$, this map shows a periodic or quasiperiodic motion depending on whether or not ω is rational. Above $k=1$, the map is noninvertible. (For a detailed discussion of this map, see [27]). All sites are updated in parallel.

The fixed point of this system is given by

$$x^* = \frac{1}{2\pi}\sin^{-1}\left(\frac{2\pi\omega}{k}\right). \qquad (3)$$

We study system using periodic boundary conditions keeping map parameters $k=1$, $\omega=0.068$ constant while varying ϵ and probability p from $[0,1]$.

In most of our studies, we have kept same value of $k=1$ and $\omega=0.068$. However, to check if some interesting phases are missing, we have performed extensive simulations by changing all parameters k, p, ω, and ϵ. We find that while there are some qualitative changes, no new phases are observed. The topological quantities such as clustering coefficient or average path length are clearly not altered when parameters other than p are changed. However, the location of dynamical phases is changed when parameters such as k, ω, or ϵ are changed. Thus, the dynamical phases and transitions between them seem to be a function of topology as well as of dynamics. We will show a dramatic example on how dynamics can change qualitatively when map parameters are changed even for same p in the latter part of the paper. The main difference between our studies with previous studies is that we do not obtain a direct (second-order) transition from a synchronized state to spatiotemporal intermittency and thus do not get a DP transition. It is possible to get such a transition on changing map parameters. However, by now, DP has been established as a paradigm for transitions to absorbing state and this has been confirmed in several studies. Hence, we restrict ourselves to the above choice of parameters and study transitions which are not studied before as dynamic phase transitions. We define an order parameter for those and even establish the validity of conventional scaling relations such as finite-size scaling and off-critical simulations. We also show that this transition cannot be explained in terms of topology alone.

III. PHASE DIAGRAM

First, we examine the system with parameters mentioned above. Many interesting phases are seen in the phase diagram displayed in Fig. 1. They are explained below.

There is a phase in which all lattice sites are synchronized and take the value of fixed point. We call it a synchronized
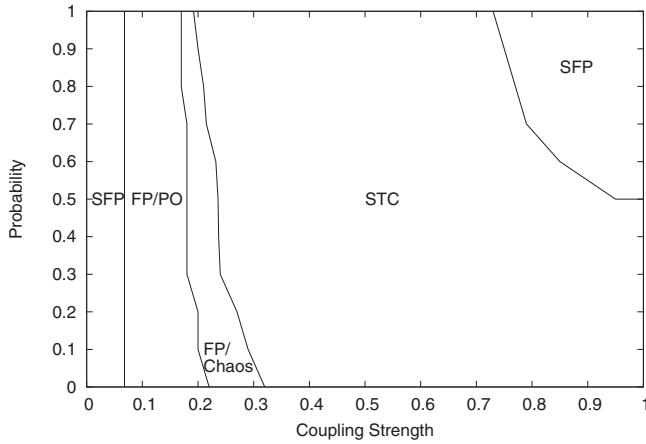
FIG. 1. Phase diagram of circle map in two parameter space of coupling strength ϵ and rewiring probability p. The abbreviations SFP, FP/PO, FP/Chaos, and STC denote synchronized fixed point, fixed point with periodic orbit, fixed point with chaos, and spatiotemporal chaos, respectively.

fixed point (SFP) phase. However, we obtain a couple of phases in which certain sites follow certain dynamics and some other sites follow different dynamics forever. For example, for higher values of couplings, we observe a phase in which some sites stay close to fixed point while the rest follow a periodic orbit. We label it as mixed phase with fixed point and periodic orbits (FP/PO). For even higher values of coupling, we observe a mixed phase with some sites stay close to the fixed point while others follow a chaotic orbit (FP/Chaos). For very strong coupling, a well-developed spatiotemporal chaos (STC) is observed. But for very large values of rewiring probability as well as coupling, system displays SFP. We never observe fully synchronized chaos or fully synchronized periodic orbit. We observe that SFP is followed by FP/PO succeeded by FP/Chaos, which is replaced by STC phases as we increase ϵ. For larger values of p, SFP reappears on increasing ϵ.

Several parts of the phase diagram are evident even by studying the bifurcation diagram of the system. Figure 2 displays the bifurcation diagram of the system for $p=0.8$. We plot the values of $x_i(t)$ after leaving sufficiently long transients as a function of ϵ. If the system reaches synchronized fixed point in a certain range of ϵ, the bifurcation diagram obviously shows only one point in that range. Similarly, one can infer that the system has reached FP/PO by observing that the diagram shows periodic orbit and a fixed point simultaneously. We have checked this statement by investigating the detailed spatiotemporal evolution of the system. Above this interval, there is a regime of FP/Chaos and STC which cannot be demarcated by using bifurcation diagram alone and we need to look into detailed spatiotemporal evolution of this system to observe this transition. Can we demarcate such transitions by looking at certain scalar order parameter? We show in next section persistence works as an excellent quantifier to describe this transition.

Obviously, looking at values of all sites in time gives little useful information and one needs to coarse-grain the system to extract useful information. Since at least a couple of phases in this system demonstrate "arrested dynamics" in the
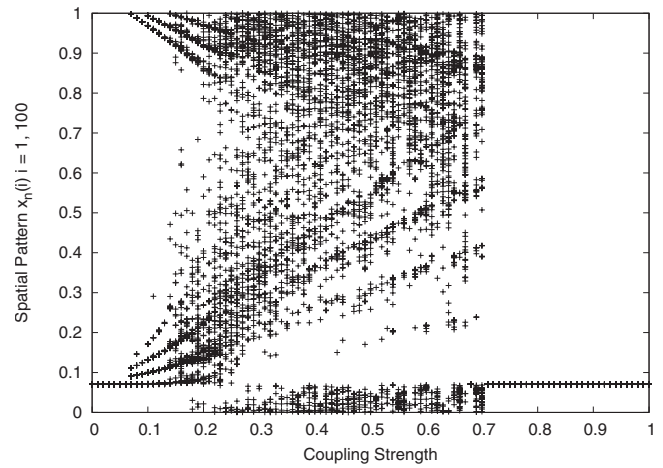

FIG. 2. Bifurcation diagram in which state variable $x_n(i)$ $(i=1,2,\ldots,100)$ has been plotted as a function of coupling strength ϵ for $p=0.8$.

sense that some sites in the lattice stay near the fixed point while others explore the other parts of phase space without infecting the laminar neighbors. We try to see the dynamics taking the fixed point as a reference point. We plot spatiotemporal space-time density plots where we distinguish between laminar and nonlaminar sites of the lattice (for FP/PO pattern) or laminar and turbulent sites of the lattice (for FP/Chaos pattern). The laminar sites are defined as those which are within distance $\delta=10^{-2}$ from the fixed point and turbulent (or nonlaminar) sites as ones which are not laminar sites. In course of time, the turbulent site may become laminar and vice versa. The spatiotemporal evolution plotted in this manner gives an idea if we have reached arrested dynamics in the sense that certain sites remain laminar forever and are not affected by their nonlaminar neighbors. This is an interesting phase which we will explore in further detail.

The spatiotemporal patterns are clearly evident from space-time density plots below. Figures 3(a)–3(d) represents a particular region in phase diagram occurring for $p=0.1$. The lattice index i is plotted along the x axis and the time index t is along the y axis. The first of these plots, Fig. 3(a), is for SFP observed at $\epsilon=0.01$, while the second, Fig. 3(b), is for ϵ values in the FP/PO phase. Figure 3(c) shows FP/chaos phase and Fig. 3(d) shows spatiotemporal chaos observed at $\epsilon=0.35$.

IV. FP/CHAOS TO SPATIOTEMPORAL CHAOS: A DYNAMIC PHASE TRANSITION

As mentioned above, we do not get a well-defined continuous transition from synchronized fixed point to spatiotemporal intermittency for our choice of parameters. However, we focus on another transition which is obtained abundantly in the phase space for our parameters. This is a transition to spatiotemporal chaos from a partially arrested phase. In this section, we critically and carefully examine the nature of transition from FP/Chaos pattern to spatiotemporal chaos. In particular, we would investigate this transition as a dynamic phase transition. In one regime, certain sites do not
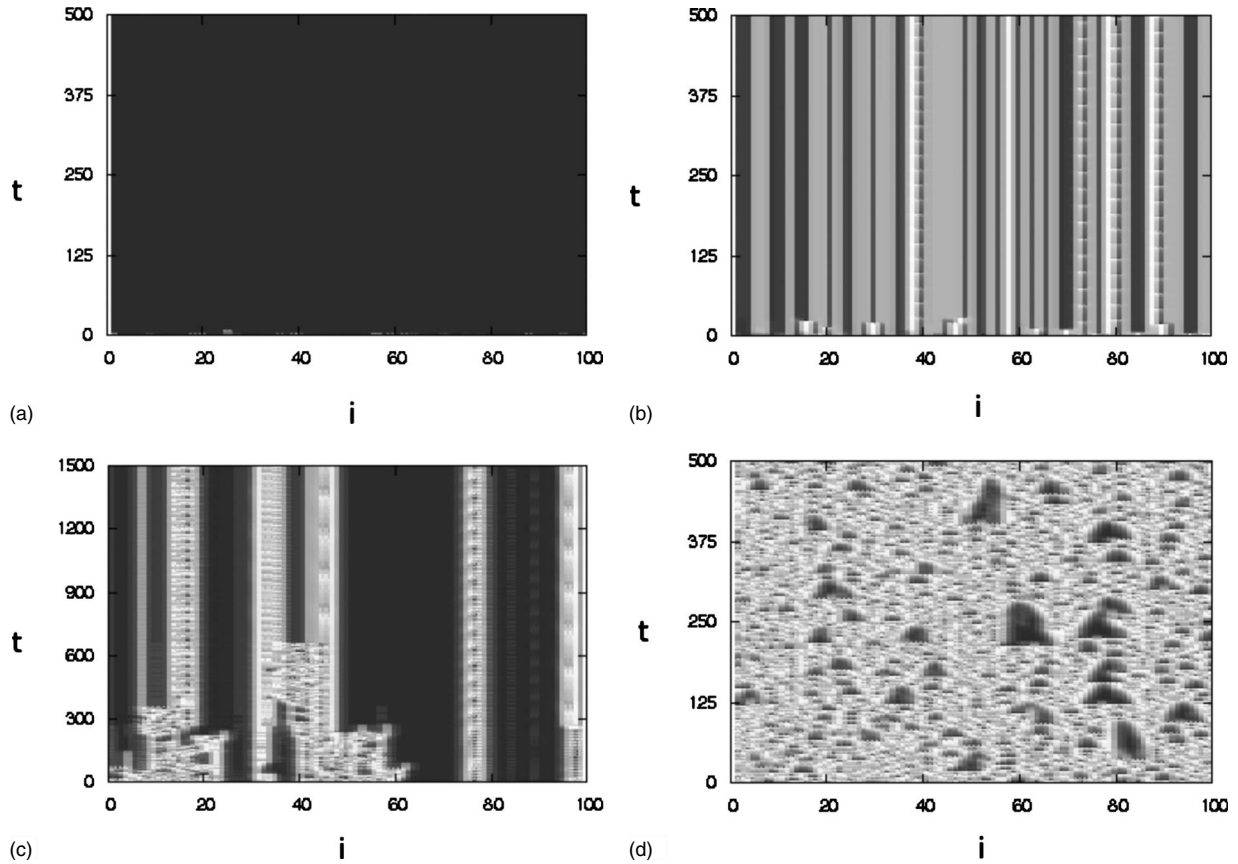
FIG. 3. Space-time plots of the different values of ϵ observed for $p=0.1$. Lattice of size 100 with parameters $\omega=0.068$ and $k=1.0$. The space-time plots show (a) in which for $\epsilon=0.01$ it shows the SFP phase, (b) is for $\epsilon=0.15$ (FP/PO phase), (c) $\epsilon=0.27$ shows a FP/Chaos phase, and (d) $\epsilon=0.35$ is in the region of spatiotemporal chaos. Laminar regions are represented by black color.

lose the memory of initial conditions even after a very long time while it is not so in the other phase. It will be of interest to investigate the role played by randomness in connections in this transition.

The order parameters which are used in previous studies in which transition to synchronized state is studied are variance of variable values in the lattice or number of active sites in a lattice. These parameters will not be able to describe this transition since these quantities will be nonzero in both arrested phase as well as case of spatiotemporal chaos. However, we find that local persistence acts as an excellent order parameter in describing this transition though it was also introduced initially in the context of transition to synchronization. In particular, Menon *et al.* introduced it in context of transition from synchronized fixed point to spatiotemporal chaos [9]. It was later found by Gade *et al.* that it works as an excellent order parameter in exploring transitions between synchronized fixed point, traveling wave state and spatiotemporal chaos in repulsively coupled CML [11]. The synchronized fixed point could be considered as state in which disturbances do not propagate in space. For our transition, disturbances do not propagate in space at least for some of the sites. Thus, local persistence could be a good quantifier. Local persistence in terms of probability is defined as follows. Persistent sites at time τ, $P(\tau)$, is a fraction of sites for which $[x_i(t)-x^*]$ did not change sign for all times $t \leq \tau$. In other words, if the site i was such that $x_i(0) < x^*$ [$x_i(0)$

$> x^*$] and it continues to have values less (greater) than x^* for all times $t \leq \tau$, then it is a persistent site. We essentially club the initial conditions assigned to various lattice sites in two groups. One set of sites having values higher than the fixed point and other set having initial condition lower than fixed point and see the conditions for which these two groups never mix. When we have a clustered state in which some sites go to fixed point while others explore a larger part of the phase space, local persistence saturates to a positive value. On the other hand, for spatiotemporal chaos, it goes to zero. Thus it has a positive value in the first phase while has a zero value asymptotically in the other phase. Clearly, it is a reasonable order parameter. In this paper, by persistence we will mean local persistence only as we do not study any other kind of persistence.

We would like to understand the nature of the phase transition which can be understood by studying the behavior of the order parameter in detail. The temporal evolution of the order parameter, the behavior of its asymptotic value as a function of control parameter, and its dependence on size of the lattice yield a valuable information which could be used to investigate the nature of this transition. In this section, we make a detailed study of behavior of persistence in the vicinity of transition between FP/Chaos and spatiotemporal chaos. The lattice size is $L=2\times10^4$. We average over 10^3 configurations.

Figures 4(a) and 4(b) show evolution of fraction of persistent sites $P(t)$ as a function of t for various values of ϵ for
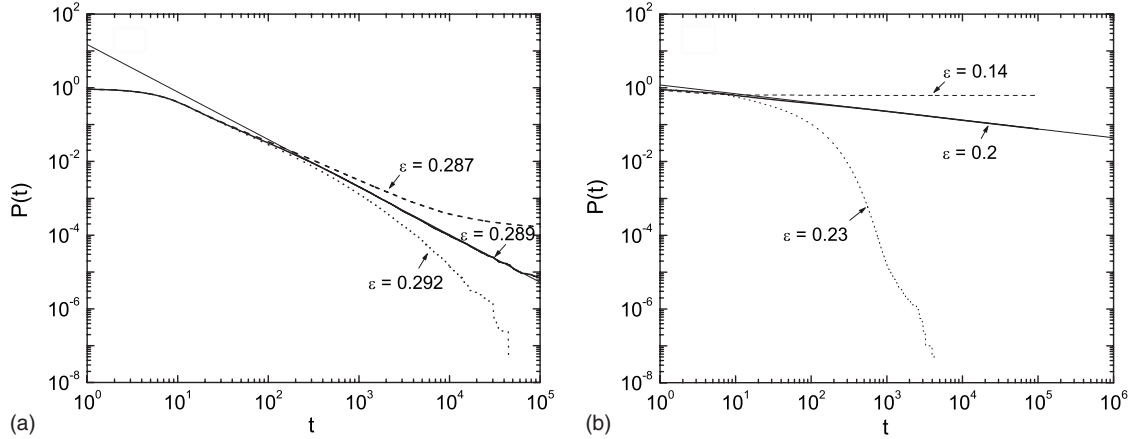
FIG. 4. Fraction of persistent sites $P(t)$ is plotted as a function of time t at the critical point which clearly displays power law. Lattice size is $L=2\times10^4$. Data are averaged over 10^3 initial conditions and critical exponents obtained are (a) 1.291 for $p=0.1$ and (b) 0.239 for $p=0.8$.

$p=0.1$ and for $p=0.8$. We observe that $P(t)$ approaches steady-state value for smaller values of coupling and exponentially decays to zero for larger values of coupling. We also observe that there is a critical value of coupling ϵ_c at which $P(t)$ goes to zero as a power law. This behavior is very similar to a prototypical second-order transition.

Though the phase transition is defined only in asymptotic time limit, there is a lot of information revealed in the manner in which order parameter decays as a function of time at the critical point. For the second-order transition, we expect it to decay as a power law and we postulate that

$$P(t) \sim 1/t^{\theta_l},\tag{4}$$

where θ_l is the critical exponent (scaling exponent). It is also known as a persistence exponent.

At the outset, we would like to note that this change in asymptotic value of persistent sites $P(\infty)$, from a positive value to zero, is strongly related to transition between FP/Chaos state and spatiotemporal chaos. The critical value ϵ_c at which a power law decay is observed, is very close to, if not the same as, the point at which transition from FP/chaos to spatiotemporal chaos occurs. (If number of laminar sites is very few and far between, persistence may still go to zero asymptotically.) We find this behavior of persistence for different rewiring probabilities p. At the transition point, a power law decay of persistence is observed. As often happens with persistence exponents, the persistence exponent is not unique or universal (see Table I). It does not show any systematic behavior as a function of p either. However, it demonstrates that not only in one dimensions (1D) or two dimensions (2D), but even for a small-world system, one can have a well-defined persistence exponent. We do get a power law decay signaling a second-order phase transition at all values of p ranging from [0,1]. Thus, transition remains continuous, though the exponents are different for different values of probability p.

A complete understanding of the critical behavior of a given system would require exact calculation of the critical exponents and of the universal scaling functions. The above power law behavior for different values of p is confirmed by phenomenological scaling law. The local persistence is expected to have a scaling of the form

$$P_l(t) \sim t^{-\theta_l}F\left(\frac{t}{L^z},t\Delta^{\nu_\parallel}\right),\tag{5}$$

where $\Delta=|\epsilon-\epsilon_c|$ is a measure of distance from the critical point, F is a scaling function, $\nu_\parallel$ is the temporal dynamical exponent, and the exponent z is related to the temporal exponent and spatial exponent [30]. In order to demonstrate the validity of this scaling form numerically, off-critical simulations and finite-size scaling are carried out.

Off-critical simulations. When the value of the control parameter differs from its critical value, the persistence does not show a power law behavior all the way. The persistence curves below (above) the critical point are expected to saturate (decay exponentially). The scaling form (5) suggests that if the values of $P(t)\Delta^{-\theta_l\nu_\parallel}$ vs $t\Delta^{\nu_\parallel}$ are plotted for different values of Δ, all curves should collapse on single curves for

TABLE I. Rewiring probability, critical coupling value, and critical exponents.

| Prob. (p)	Critical point (ϵ_c)	Persistence exponent (θ_l)	$\nu_\parallel$	z
0.0	0.31799 ± 0.00002	1.565 ± 0.003	1.293 ± 0.003	1.145 ± 0.003
0.1	0.289 ± 0.0002	1.291 ± 0.004	1.60 ± 0.02	1.085 ± 0.003
0.2	0.271 ± 0.0002	1.247 ± 0.003	1.82 ± 0.02	1.146 ± 0.002
0.3	0.2348 ± 0.0001	0.344 ± 0.002	1.84 ± 0.02	1.650 ± 0.003
0.4	0.2330 ± 0.0003	0.670 ± 0.002	1.13 ± 0.01	2.134 ± 0.002
0.5	0.2360 ± 0.0003	1.775 ± 0.002	0.65 ± 0.02	4.70 ± 0.03
0.6	0.2358 ± 0.0002	1.510 ± 0.002	0.93 ± 0.02	3.50 ± 0.02
0.7	0.2140 ± 0.0003	0.461 ± 0.002	0.20 ± 0.02	1.586 ± 0.002
0.8	0.200 ± 0.003	0.239 ± 0.002	0.470 ± 0.003	1.786 ± 0.002
0.9	0.192 ± 0.002	0.149 ± 0.001	0.70 ± 0.02	2.13 ± 0.02
1.0	0.190 ± 0.001	0.115 ± 0.001	0.45 ± 0.02	2.33 ± 0.03
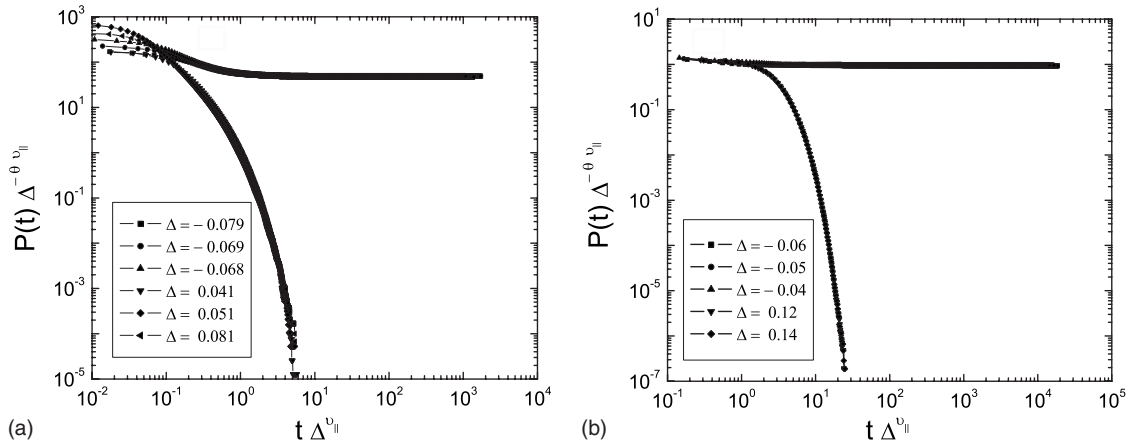
FIG. 5. Off-critical simulations near critical point. The graph demonstrates data collapse according to the scaling form (5). Lattice size $L=2\times10^4$. We averaged over 500 initial conditions. (a) is for $p=0.1$ and (b) for $p=0.8$.

the correct choice of $\nu_{\parallel}$. Figures 5(a) and 5(b) shows that the best data collapse is obtained when $\nu_{\parallel}=1.60$ and 0.47 for $p=0.1$ and 0.8, respectively. Similarly, off-critical simulations are carried out for all probabilities. We try to get scaling collapse which allows us to find values of $\nu_{\parallel}$ for different values of p.

Finite-size scaling. To compute dynamic exponent z, it is necessary to carry out finite-size scaling. For values of parameters close to the critical point, the finite-size effects can be noticed. We measure the critical point for $L=2\times10^4$. This lattice size is large enough that the finite-size effects could be ignored and this critical point could be treated as asymptotic critical point ϵ_c. $P(t)$ is computed as a function of t at $\epsilon=\epsilon_c$ for various values of L ranging from 100 to 400. $P(t)L^{\theta_l z}$ is plotted against t/L^z. For a correct choice of z, it is expected the data obtained for different lattice sizes should collapse onto a single curve. We find that this is indeed true. This scaling collapse is demonstrated in Figs. 6(a) and 6(b) for $p=0.1$ and $p=0.8$, respectively. Similarly, finite-size scaling is carried out for several values of p ranging from [0,1].

The local slope analysis of persistent exponent for $p=0.8$ shown in Fig. 7 depicts the exponent $\theta_l=0.239$ which remains constant for a large range after initial transients are

over. Thus, we conclude that the local persistence exponent $\theta_l=0.239$ obtained is fairly accurate.

A systematic study of transition for all probabilities resulted in excellent scaling collapse near critical point for all these cases, revealing a second-order transition. The values of exponents have been calculated and presented in Table I below. In this table, the values of critical point, persistence exponent, and dynamic exponents $\nu_{\parallel}$ and z for all probabilities are given. It is clear that while critical value of probability goes down monotonically for higher rewiring probability p, the exponents do not show any particular pattern in general.

V. COMPLEX INTERPLAY OF DYNAMICS AND TOPOLOGY

Since the above studies present a rather complex picture in which the persistence exponents do not show any systematic behavior, one would wonder if there is a way to understand those by studying properties of underlying lattice such as average path length or clustering coefficient. Unfortunately, it turns out that topology alone does not dictate the value of exponent. Apart from the case of $k=1$, $p=0.1$ stud-
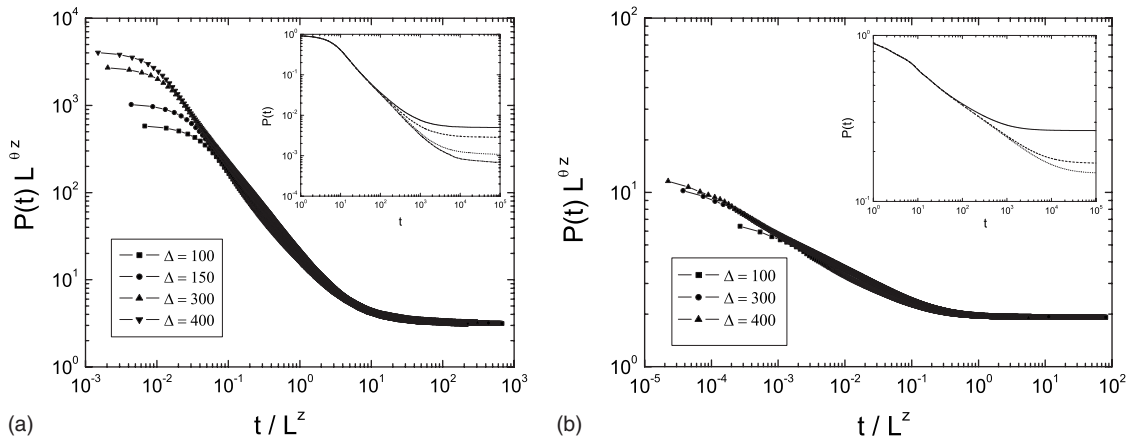

FIG. 6. Finite-size scaling for different lattice sizes. (a) $L=100, 150, 300,$ and 400 for $p=0.1$ and (b) $L=100, 300,$ and 400 for $p=0.8$. The graph demonstrates data collapse according to the scaling form in Eq. (5).
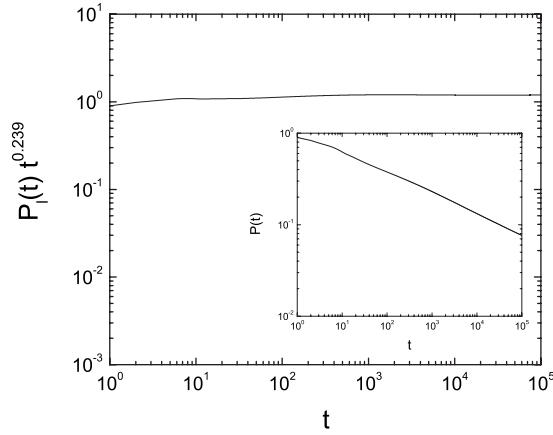
FIG. 7. The plot shows $P_l(t)$ multiplied by $t^{-\theta_l}$ with θ_l=0.239 for p=0.8. Inset shows the raw data of the simulation.

ied above, let us consider two cases k=0.8, p=0.1 and k=1.3, p=0.1. In these cases, p is kept constant leaving various topological properties unchanged. In all these cases, a transition from clustered phase to spatiotemporal chaos is obtained. However, if we look at the persistence exponent, we get exponent 1.155 ± 0.002 at critical point ϵ_c =0.1784 ± 0.0002 for k=0.8 [Fig. 8(a)]. As mentioned above, for k=1, the exponent is 1.291 ± 0.004. The difference of the exponents for k=1 and k=0.8 is much more than our error bar. Now let us consider case k=1.3. We have given plots of $P(t)$ as a function of t for two values of ϵ below and above transition [Fig. 8(b)]. The curve at critical point will be bounded by these two curves. Here, a steep decay in persistence is seen by 3 decades if time is increased by 1 decade. Thus the persistence exponent is between 2.7 and 3.3 for k=1.3 if this transition is classified as a second-order transition. These dramatic changes in behavior of persistence occur when we change only map parameters and coupling, leaving p unchanged implies that exponent is a function of p which dictates topology as well as of map parameters which affect dynamics.
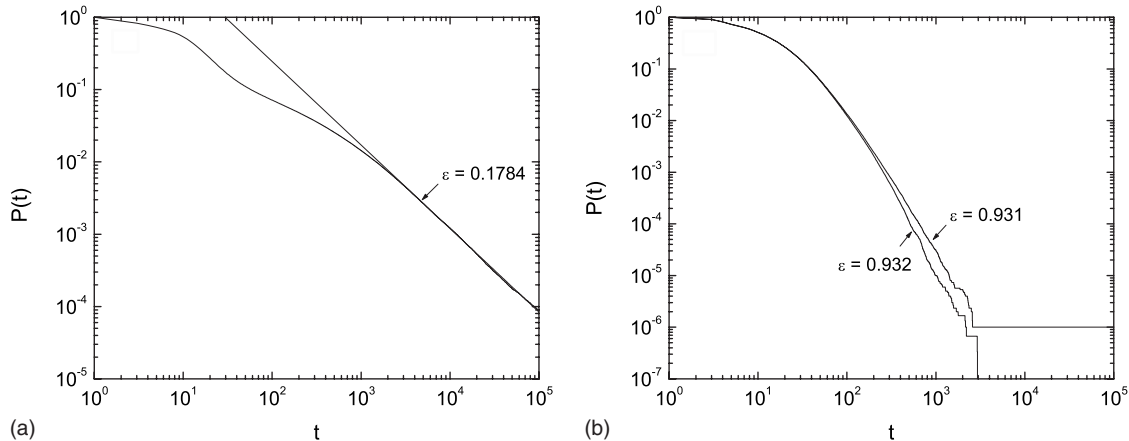
VI. CONCLUSION

We have studied the spatiotemporal patterns of the system on small-world network with varying probability p and varying ϵ from [0,1]. Also studied the phase diagram and the bifurcation diagram, which clearly show various phases of system. We find that persistence $P(t)$ acts as an excellent order parameter for transition from FP/Chaos to STC. Thus persistence could be a useful quantifier to study even for transitions other than transition to a synchronized state. We go beyond this and establish applicability of usual scaling ansatz about finite-size scaling and off-critical simulations in this work. This transition is continuous and $P(t)$ displays a power-law decay at critical point for all probability p. The persistence exponents are different for different values of p. (They could also be different if we retain same p and change map parameters.) We have shown excellent scaling collapses and demonstrated that the conventional scaling holds also for small-world lattices. Unfortunately, analytical derivation of persistence exponent has been carried out only in simplest of cases and even in those cases it is a very complicated derivation since persistence exponents require knowledge of time correlations of arbitrary order. Nonetheless, this work clearly demonstrates that though the exponent is nonuniversal, persistence is an useful order parameter for the transition from a clustered state to spatiotemporal chaos, revealing a second-order transition. We have illustrated that topology alone does not dictate the value of persistence exponent. In particular, we have shown that exponent could be different when map parameter for the same value of p is changed. This implies that one needs to be very careful in dynamic phase transitions in nonequilibrium systems where the dynamics plays as important role as topology. This also shows that persistence could be a useful order parameter for studying transition from a jammed or arrested phase to a phase where disturbances move freely in the space.

FIG. 8. Persistence $P(t)$ is plotted as a function of time t for p=0.1. Lattice size L=2×10^4. We averaged over 500 initial conditions. (a) The exponent is 1.155 for k=0.8. (b) The exponent is between 2.7 and 3.3 for k=1.3.

[1] A. Aceves, H. Adachihara, C. Jones, J. C. Lerman, J. Moloney, D. McLaughlin, and A. C. Newell, Physica D **18**, 85 (1986).

[2] Y. Kuramoto, *Chemical Oscillations, Waves and Turbulence* (Springer, New York, 1984).

[3] J.-R. Chazottes and B. Fernandez, *Dynamics of Coupled Map Lattices and of Related Spatially Extended Dynamical Systems* (Springer, New York, 2004).

[4] B. Chopard and M. Droz, *Cellular Automata Modeling of Physical Systems* (Cambridge University Press, London, 1998).

[5] K. Kaneko, *Theory and Applications of Coupled Map Lattices* (Wiley, New York, 1993).

[6] A. Pikovsky, M. Rosenblum, and J. Kurths, *Synchronization: A Universal Concept in Nonlinear Sceiences* (Cambridge University Press, London, 2001).

[7] N. Chatterjee and N. Gupte, Phys. Rev. E **53**, 4457 (1996).

[8] T. M. Janaki, S. Sinha, and N. Gupte, Phys. Rev. E **67**, 056218 (2003).

[9] G. I. Menon, S. Sinha, and P. Ray, Europhys. Lett. **61**, 27 (2003).

[10] Z. Jabeen and N. Gupte, Phys. Rev. E **72**, 016202 (2005).

[11] P. M. Gade, D. V. Senthilkumar, S. Barve, and S. Sinha, Phys. Rev. E **75**, 066208 (2007).

[12] K. Kaneko, Physica D **54**, 5 (1991).

[13] D. J. Watts and S. H. Strogatz, Nature (London) **393**, 440 (1998).

[14] A.-L. Barabási and E. Bonabeau, Sci. Am. **288**, 60 (2003).

[15] R. Albert and A.-L. Barabási, Rev. Mod. Phys. **74**, 47 (2002).

[16] R. J. Baxter, *Exactly Solved Model in Statistical Mechanics* (Academic Press, London, 1982).

[17] P. M. Gade and S. Sinha, Phys. Rev. E **72**, 052903 (2005).

[18] C. Moore and M. E. J. Newman, Phys. Rev. E **61**, 5678 (2000).

[19] C. Moore and M. E. J. Newman, Phys. Rev. E **62**, 7059 (2000).

[20] K. Medvedyeva, P. Holme, P. Minnhagen, and B. J. Kim, Phys. Rev. E **67**, 036118 (2003).

[21] B. J. Kim, H. Hong, P. Holme, G. S. Jeon, P. Minnhagen, and M. Y. Choi, Phys. Rev. E **64**, 056135 (2001).

[22] H. Hong, B. J. Kim, and M. Y. Choi, Phys. Rev. E **66**, 018101 (2002).

[23] M. Kuperman and G. Abramson, Phys. Rev. E **64**, 047103 (2001).

[24] S. Sinha, Phys. Rev. E **66**, 016209 (2002).

[25] P. M. Gade and S. Sinha, Int. J. Bifurcation Chaos Appl. Sci. Eng. **16**, 2767 (2006).

[26] R. C. Hilborn, *Chaos and Nonlinear Dynamics*, 2nd ed. (Oxford University Press, Oxford, 2000).

[27] M. H. Jensen, P. Bak, and T. Bohr, Phys. Rev. A **30**, 1960 (1984).

[28] M. E. J. Newman, J. Stat. Phys. **101**, 819 (2000).

[29] J. M. Kleinberg, Nature (London) **406**, 845 (2000).

[30] J. Fuchs, J. Schelter, F. Ginelli, and H. Hinrichsen, J. Stat. Mech.: Theory Exp. (2008), P04015.